

# Rotationally induced Penning ionization of ultracold photoassociated helium dimers

J. LÉONARD<sup>1</sup> (\*), A. P. MOSK<sup>1</sup> (\*\*), M. WALHOUT<sup>1</sup>(\*\*\*), M. LEDUC<sup>1</sup>,  
M. VAN RIJNBACH<sup>2</sup>, D. NEHARI<sup>2</sup> and P. VAN DER STRATEN<sup>2</sup>

<sup>1</sup> *Ecole Normale Supérieure and Collège de France, Laboratoire Kastler Brossel -  
24 rue Lhomond, 75231 Paris Cedex 05, France.*

<sup>2</sup> *Debye Institute, Atom Optics and Ultrafast Dynamics, Utrecht University -  
P.O. Box 80,000, 3508 TA Utrecht, The Netherlands.*

PACS. 33.20.-t – Molecular spectra.

PACS. 34.50.Gb – Electronic excitation and ionization of molecules.

PACS. 34.20.Cf – Interatomic potentials and forces.

## Abstract. –

We have studied photoassociation of metastable  $2^3S_1$  helium atoms near the  $2^3S_1$ - $2^3P_2$  asymptote by both ion detection in a magneto-optical trap and trap-loss measurements in a magnetic trap. A detailed comparison between the results of the two experiments gives insight into the mechanism of the Penning ionization process. We have identified four series of resonances corresponding to vibrational molecular levels belonging to different rotational states in two potentials. The corresponding spin states become quasi-purely quintet at small interatomic distance, and Penning ionization is inhibited by spin conservation rules. Only a weak rotational coupling is responsible for the contamination by singlet spin states leading to a detectable ion signal. However, for one of these series Bose statistics does not enable the rotational coupling and the series detected through trap-loss does not give rise to sufficient ionization for detection.

Recently there have been many experimental efforts to achieve Bose-Einstein condensation (BEC) for metastable rare-gas atoms [1–5]. The achievement of BEC with ultracold metastable  $^4\text{He}(2^3S_1)$  atoms ( $\text{He}^*$ ) [1, 2] followed the prediction [6, 7] that spin conservation prohibits Penning ionization in the fully stretched molecular spin state and thus prevents the cold cloud of spin-polarized metastable atoms to ionize before it Bose condenses. By contrast, Penning ionization is less effectively suppressed in heavier rare gases, which must be trapped in a metastable  $^3P$  state and are therefore subject to stronger spin-orbit collisional couplings [8]. In this context, there is general interest in both experimental and theoretical studies of the dynamics that lead to Penning ionization and its suppression in trapped metastable rare gases. For a magnetically trapped sample in the  $\text{He}^*$  state, the common spin orientation imposes a strict conservation rule that permits collisional Penning ionization ( $\text{He}^*(2^3S_1) + \text{He}^*(2^3S_1) \rightarrow$

(\*) Permanent address: Institut de Physique et Chimie des Matériaux de Strasbourg, France.

(\*\*) Permanent address: Dept. of Science & Technology and MESA+ research institute, University of Twente, The Netherlands.

(\*\*\*) Permanent address: Calvin College, Grand Rapids, MI, USA.

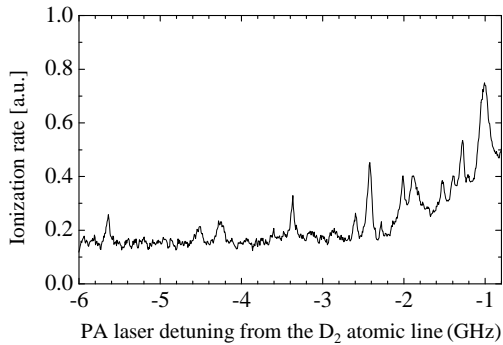


Fig. 1

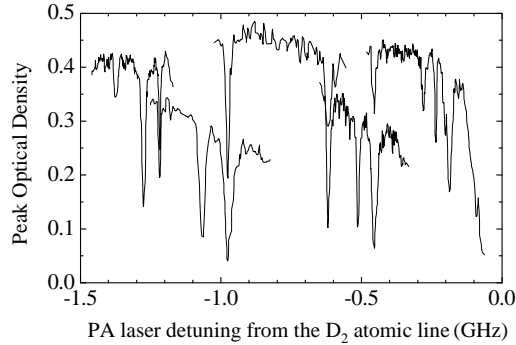


Fig. 2

Fig. 1 – Typical data from the Utrecht Magneto-Optical Trap (MOT) experiment: ionization rate versus detuning of the PA laser from the  $D_2$  atomic line. This spectrum is the result of the average over 20 scans. The PA laser intensity is  $10^4 I_{sat}$ .

Fig. 2 – Typical data from the ENS magnetic trap experiment: optical density versus detuning of the PA laser from the  $D_2$  atomic line. The drops in peak optical density result both from trap loss and temperature increase of the sample. The five spectra displayed are obtained with different PA laser exposure times (from 30 ms to 150 ms) and intensities (from  $3I_{sat}$  to  $I_{sat}/10$ ). Each spectrum is a series of up to 500 individual data points smoothed by averaging over 5 adjacent points.

$\text{He}[1^1S] + \text{He}^+ + e^-$ ) only through a spin-dipole coupling that is relatively weak [9]. The goal of this paper is to discuss the mechanism leading to Penning ionization that we have observed in our photoassociation experiments with helium. Through a detailed comparison between data from two qualitatively different experiments, we show that weak couplings induced by molecular rotation can lead to the ionization of photoassociated molecules.

We have performed complementary photoassociation (PA) experiments close to the  $2^3S_1$ - $2^3P_2$  asymptote in Utrecht [10,11] and Paris [12]. In the experiments we observe a molecular spectrum of photoassociation resonances up to 10 GHz below the asymptote. Our ability to interpret the molecular spectrum depends critically on the fact that we use different methods of trapping and detection in the two experiments. In Utrecht a MOT operated at a wavelength of  $1.083 \mu\text{m}$  is used to accumulate typically a few  $10^6$   $\text{He}^*$  atoms at a temperature of  $\sim 1.9$  mK and a density of order  $10^{10} \text{cm}^{-3}$ . The accumulation of the PA spectrum is done by pulsing the frequency of the MOT beams from the optimized trapping frequency to far off-resonance (about 200 natural linewidths) at the rate of 25 kHz with a duty cycle of 50 % and shining the PA laser during the off-resonant periods. When scanning the PA laser frequency, PA resonances are detected as peaks in the ion production rate, which is measured with a multichannel plate (MCP). Thus, this experiment is extremely sensitive to those excited states that predominantly decay by Penning ionization. Fig. 1 shows a typical spectrum obtained after averaging over 20 scans. The high rate at which the MOT and PA lasers are pulsed allows for a fast accumulation of the PA spectrum over broad frequency ranges (from 0 to 20 GHz below the  $D_2$  line). Since the clouds are unpolarized, the PA laser can excite molecular states corresponding to both *gerade* and *ungerade* symmetries.

In Paris typically  $5 \times 10^8$  atoms are loaded in a magnetic trap from a MOT operating at  $1.083 \mu\text{m}$ . Forced evaporative cooling is used to bring the spin-polarized cloud to densities of  $10^{13} \text{cm}^{-3}$  and temperatures of typically  $10 \mu\text{K}$  or lower, that is to say slightly above the critical temperature for BEC. The cloud containing a few  $10^6$  atoms is then illuminated by a

PA light pulse, released from the trap and destructively imaged to determine its density and temperature. PA resonances induce loss in the magnetic trap, which can be caused both by enhanced Penning ionization through the excited molecular state and by radiative decay of the molecule produced. A significant heating is also observed which can be monitored as a signature of a PA resonance. In this experiment, a new cloud has to be trapped, cooled down and detected for each new choice of the PA laser frequency. Therefore, the PA spectrum can only be accumulated over small ranges of frequency since the rate of accumulation of the PA spectrum is of order 1/30 Hz instead of 25 kHz in the Utrecht experiment. Such a difference in the experimental procedures comes from the much lower detection efficiency offered by absorption imaging at 1.083  $\mu\text{m}$  compared to ionization rate measurement. In Paris, parts of the spectrum between 0 and 14 GHz below the D2 line have been recorded. Fig. 2 shows a set of typical spectra. Since pairs of spin-polarized  $\text{He}^*$  atoms interact through the *gerade*  $^5\Sigma_g^+$  state, only *ungerade* molecular states can be excited by photoassociation.

In both experiments, discrete PA resonances are observed on top of a broad non-resonant ionization or loss signal which becomes dominant at high laser intensities and/or small detunings (see fig. 1 and 2). Although densities are  $10^3$  times higher and temperatures nearly  $10^3$  times lower in the magnetic trap compared with those in the MOT, we find that most of the resonance lines in the frequency range of 0-14 GHz below the  $2^3S_1+2^3P_2$  atomic transition appear in both experiments. The PA lines are narrower in the Paris experiment because there is no power broadening, unlike in the Utrecht Experiment. In the present analysis we will be primarily concerned with discrete line positions. We estimate a 10-20 MHz uncertainty for each line position in both experiments due to the uncertainty in determining the detuning from atomic resonance using a Fabry-Perot interferometer. This level of precision is sufficient for a detailed comparison between the two sets of data and with our calculated molecular potentials. The energies of the resonances which appear in both experiments are in full agreement within the experimental uncertainties [13]. However, a few PA resonances are observed in ionization rate detection but not in trap loss. We attribute these to *gerade* excited state potentials not accessible from spin-polarized atoms, and we will not discuss them in this paper. Conversely, and more interestingly, a few PA resonances appear only in the trap loss data and not in the ion data. They bring a new insight in the mechanism of ionization of these molecules as we shall see below.

We are concerned here by the PA molecular lines corresponding to the *ungerade* excited states near the  $2^3S_1+2^3P_2$  asymptote. Only 27 molecular *ungerade* potentials are asymptotically connected to the pair  $2^3S_1+2^3P_{0,1,2}$ . The long range tail of these potentials can be calculated using perturbation theory [11, 14]. The resonant retarded dipole-dipole interaction ( $C_3/R^3$ ) and the atomic fine structure interaction are treated as a perturbation of a pair of non-relativistic atoms with a fixed internuclear distance  $R$ . This approach is clearly valid only for large  $R$ , where short-range molecular interactions can be neglected. The analysis shows that some purely long-range potentials are present near the  $2^3S_1+2^3P_{0,1}$  asymptotes, for which it is sufficient to treat molecular rotation and vibration only as diagonal (first-order) corrections to the electronic interaction [12, 14, 15]. However, below the  $2^3S_1+2^3P_2$  asymptote, all the molecular potentials have a short range part which is not calculated here. The  $C_6$  coefficients for the  $\Sigma$  and  $\Pi$  electronic states are included in the electronic interaction, based on the values reported by Venturi *et al.* [15], but higher-order dispersion terms are neglected. The potentials of interest for the interpretation of the *ungerade* spectrum are shown in fig. 3. Only 8 *ungerade* potentials have an attractive long-range behavior. Only 4 of these potentials (displayed in solid line in fig. 3) have significant quintet spin character at short distance and are expected to give rise to narrow PA resonances since this stretched state of angular momentum is subject to the same spin-conservation rule that prevents ionization in a polarized gas

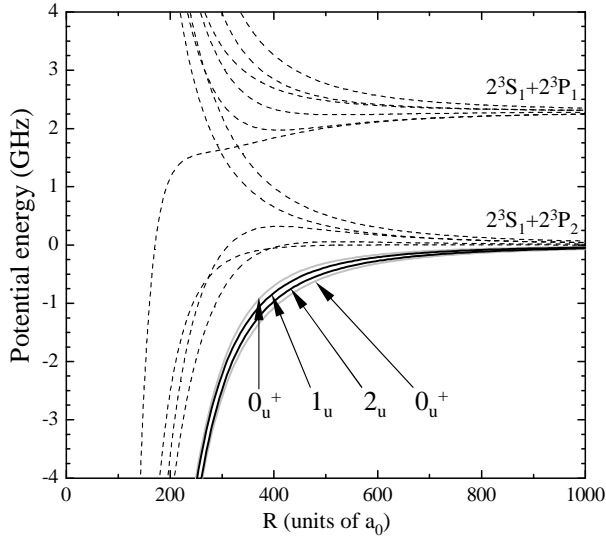


Fig. 3

Fig. 3 – *Ungerade* Hund’s case (c) potentials around the  $2^3S_1-2^3P_2$  asymptote. The dashed attractive potential curves correspond to short-range triplet molecular spin states which are expected to autoionize via the Penning mechanism. The grey solid lines are the attractive  $0_u^+$  states which have partly quintet and partly singlet spin-character at short interatomic distance. The black solid lines indicate the  $1_u$  and  $2_u$  states which become purely quintet at short range.

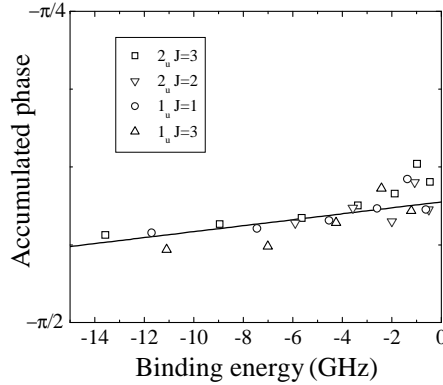


Fig. 4

Fig. 4 – The accumulated phase of the four series of resonances as a function of detuning  $\Delta\nu$ . The resonances correspond to molecular states which all become  $5\Sigma_u^+$  at short interatomic distance.

of metastable helium atoms [6]. For molecular spin states which are purely triplet or singlet at short interatomic distance, the ionization probability is so large that such a molecule would hardly survive half an oscillation period. Consequently, there is a priori no series of discrete bound states (*i.e.* no molecule) to be expected with strong triplet or singlet spin character.

In order to assign the PA lines to one or several of the attractive, *ungerade* molecular potentials near the  $2^3S_1-2^3P_2$ , we use the accumulated phase method [16]. Wavefunctions corresponding to a given electronic state but different (small) binding energies and different (small) angular momenta should all be in phase at short enough interatomic distance. In practice, we integrate inwards single-channel radial Schrödinger equations for each of the 8 attractive molecular potentials and for each of the energies determined experimentally for the PA resonances:

$$\left\{ -\frac{\hbar^2}{m} \frac{d^2}{dr^2} + V_{J,\Omega_u}(r) - E_{res} \right\} u(R) = 0.$$

Here  $m$  is the mass of  $^4\text{He}$ ,  $E_{res}$  is the energy of one of the resonances detected.  $V_{J,\Omega_u}(r)$  is the effective long-range interaction potential corresponding to a given  $\Omega_u$  *ungerade* electronic state and a given rotational state  $J$  when neglecting non-diagonal rotational couplings between  $\Omega$  and  $\Omega \pm 1$  subspaces [14, 17]. We then compute the phases  $\Phi(r)$  accumulated by the wavefunctions  $u(r)$  at the interatomic distance  $r_{in} = 20 a_0$ . At this distance, the binding energy and rotational energy are much smaller than the interaction energy between the two nuclei and the assumption of stationarity of the accumulated phase is valid. In addition, the vibrational motion of the molecule is quasi-classical and the accumulated phases can be

TABLE I – Measured binding energies for the ungerade molecular states observed in the Utrecht and ENS experiments. Four series of PA resonances are identified which correspond to vibrational levels belonging to different rotational states in two electronic potentials:  $J = 2$  and  $J = 3$  in  $2_u$ , and  $J = 1$  and  $J = 3$  in  $1_u$ . The \* signs indicate resonances which are not detected in Utrecht by ionization-rate monitoring. All the other lines presented here are observed in both experiment at the same detuning within the experimental uncertainties of 20 MHz in both cases. Energies are given in GHz with respect to the  $D_2$  atomic line.

	$2_u$ $J = 2$	$2_u$ $J = 3$		$1_u$ $J = 1$	$1_u$ $J = 3$
$v$	-0.51*	-0.455	$v'$	-0.62	
$v - 1$	-1.07*	-0.98	$v' - 1$	-1.37	-1.22
$v - 2$	-2.00*	-1.88	$v' - 2$	-2.59	-2.42
$v - 3$	-3.57*	-3.37	$v' - 3$	-4.53	-4.25
$v - 4$	-5.90*	-5.64	$v' - 4$	-7.45	-7.01
$v - 5$		-8.95	$v' - 5$	-11.70	-11.10
$v - 6$		-13.56	$v' - 6$		

written as

$$\Phi(r) \simeq \arctan \left[ \sqrt{m(E_{res} - V_{J,\Omega_u}(r)) / (\hbar \partial \ln u(r) / \partial r)} \right].$$

We plot for each effective potential the accumulated phases as a function of the PA laser detuning  $\Delta\nu$  of the resonances and we search for series of resonances with nearly equal phases. According to the assumption above, these series correspond to molecular levels in the same potential with the same  $J$ , but increasing vibrational number. This way we are able to identify 23 resonances in four series as reported in Table I. The result of the identification does not depend sensitively on our choice of  $r_{in}$  between 15 and 30  $a_0$ . The series found to have a common accumulated phase correspond to the vibrational progressions of the Hund's case (c)  $1_u$  ( $J=1,3$ ) and  $2_u$  ( $J=2,3$ ) states.

It turns out that the four series of resonances identified correspond to molecular states which all become  ${}^5\Sigma_u^+$  with purely quintet spin character at short range, and hence have the same short-range interaction potential. Therefore the four corresponding accumulated phases should all be equal. This is confirmed by plotting on a same graph the accumulated phases versus detuning for the four series identified as shown in fig. 4, where all resonances belonging to one series are indicated with the same symbol. A linear fit of the whole set of points in fig. 4 gives the residual dependence of the optimal accumulated phase with the energy  $E$ :  $\Phi(r_{in}) \simeq -1.30(2) + 0.0036(20) \times E$ . Note that the actual value of the optimal accumulated phase is a priori wrong since the potentials we use are only valid at long range and certainly not at distances as small as  $r_{in} = 20 a_0$ . However, the only requirement for the method to work is that the interaction potentials are exact at long interatomic distances where the calculated wavefunctions are no longer in phase with each other.

The most important result of the comparison between the two experiments is that the series of  $2_u$  ( $J=2$ ) is missing in the ionization data, whereas the other three series have been detected in both experiments. Non-diagonal coupling between the  $\Omega$  subspaces should be considered in detail in order to understand this fact. The  $1_u$  and  $2_u$  potentials are close in energy from two  $0_u^+$  potentials over a large range of internuclear distances (see fig. 3). The two  $0_u^+$  potentials connect for a significant part to the  ${}^1\Sigma_u^+$  potential at short range, which gives rise to ionization. By contrast, the  $1_u$  and  $2_u$  become purely quintet, and hence the Penning ionization process is largely inhibited as already mentioned. However, accurate description

shows that molecular rotation couples  $1_u$  to  $0_u^+$  as well as  $2_u$  to  $0_u^+$  (to the second order, via the nearby  $1_u$  state), allowing for some ionization probability of the  $1_u$  and  $2_u$  states.

Given the properties of the  $0_u^+$  states with respect to the inversion ( $u/g$ ) and reflection ( $\pm$ ) symmetries, Bose statistics ( $\text{He}^*$  and its nuclei are bosons) imposes that the rotational quantum number  $J$  must be odd for  $0_u^+$  states [18]. Therefore the non-diagonal rotational coupling to a  $0_u^+$  state can only be effective for odd values of  $J$ . Hence, at short distance  $1_u$   $J = 2$  and  $2_u$   $J = 2$  remain purely quintet whereas  $1_u$   $J = 1, 3$  and  $2_u$   $J = 3$  are contaminated by non quintet spin states through the coupling to  $0_u^+$   $J = 1$  and  $J = 3$ . This explains why ion detection is only possible for  $1_u$   $J = 1, 3$  and  $2_u$   $J = 3$  whereas  $1_u$   $J = 2$  and  $2_u$   $J = 2$  produce no detectable ions in the Utrecht Experiment. The  $2_u$   $J = 2$  resonances appear only in the ENS experiment with an intensity comparable to that of the other 3 series. The  $1_u$   $J = 2$  is not detected in the Paris experiment with a significant signal to noise ratio. However, based on the above analysis, one resonance observed at -1.27(2) GHz in the spectrum obtained at ENS could possibly be assigned to the  $1_u$   $J = 2$  series. Other resonances belonging to the same series are expected at frequencies which were either not scanned at all at ENS or scanned in a preliminary experiment with reduced sensitivity, which means that the intensity of those resonances should be at least 5 to 10 times less than the other resonances detected. Finally, all the resonances observed in Paris [19] are identified by this analysis except those which appear at detunings smaller than -0.28 GHz for which the accuracy of the frequency measurement (20 MHz) does not allow for an accurate determination of the corresponding accumulated phases. As expected, no resonance has been observed with a non-quintet spin state at short interatomic range.

In the Utrecht experiment, the signal-to-noise ratio vanishes when the detuning is increased and no PA resonance has been observed at detunings larger than -13.56 GHz. In the ENS experiment, no systematic scan is possible at large detunings due to the small rate of data accumulation. Therefore the observation of resonances detuned further from resonance is only possible if their position is predicted. The PA line intensities are modulated by the amplitude of the ground state radial wavefunction [20] and one can expect a vanishing line intensity for excited bound states having their outer turning points  $R_{out} \simeq a$ , where  $a = 200 \pm 40 a_0$  is the s-wave scattering length [21]. This corresponds to PA resonances in the range -5 GHz to -15 GHz. Deeper bound states (with  $R_{out} < a$ ) should instead lead to detectable PA resonances. These bound states might prove useful as intermediate excited states for driving two-photon transitions from a free pair of atoms to a bound pair in the ground state  $^5\Sigma_g^+$ . Indeed, deeper excited bound states have better Franck-Condon overlap with the final bound state. In addition the background non-resonant ionization reduces with increasing detuning.

From the present analysis we can conclude, that the ionization and trap loss experiments yield complementary information on the photoassociation of the  $\text{He}^*\text{-He}^*$  system on the  $2^3S_1$ - $2^3P_2$  transition [22]. We have been able to identify four series of resonances and indicated why those series have a small ionization probability. Of the four series, one series is only seen in the trap loss experiment. The most striking point out of this study is, that this  $2_u$  ( $J = 2$ ) potential cannot couple by rotational coupling to potentials, which have a large ionization probability. Thus, a molecule in this potential preferentially decays radiatively. This study might play an important role in future two-photon PA experiments to be done in Paris for an accurate determination of the elastic scattering length for the  $\text{He}^*\text{-He}^*$  system. Indeed, we can use the potential curves and the accumulated phase determined in the present analysis, to predict the position of the lower-lying bound states in the  $1_u$  and  $2_u$  potentials. These states are only accessible experimentally if one approximately knows where to look for them, given the low rate of accumulation of the data in the experiment of ENS. They might prove to have good Franck-Condon overlap with the least-bound state in the ground-state potential,

which is of crucial importance to drive two-photon transitions in the view of measuring the scattering length of spin-polarised metastable helium.

The work of the Utrecht group has been supported by the “Stichting voor Fundamenteel Onderzoek der Materie (FOM)”, which is financially supported by the “Nederlandse organisatie voor Wetenschappelijk Onderzoek (NWO)”. DN is supported by the EU research training network “Cold molecules” (COMOL), under the contract number HPRN-2002-00290.

## REFERENCES

- [1] A. Robert, *et al.*, *Science* **292**, 461 (2001).
- [2] F. Pereira Dos Santos, *et al.*, *Phys. Rev. Lett.* **86**, 3459-3462 (2001).
- [3] P.J.J. Tol, *et al.*, *Phys. Rev. A* **60**, R761 (1999).
- [4] S. J. M. Kuppens, *et al.*, *Phys. Rev. A* **65**, 023410 (2002).
- [5] M. Zinner, *et al.*, *Phys. Rev. A* **67**, 010501 (2003).
- [6] L. Shearer and L. Riseberg, *Phys. Lett.* **33A**, 325 (1970).
- [7] M.W. Müller, *et al.*, *Z. Phys. D* **21**, 89 (1991).
- [8] M.R. Doery, *et al.*, *Phys. Rev. A* **58**, 3673-3682 (1998).
- [9] G.V. Shlyapnikov, *et al.*, *Phys. Rev. Lett.* **73**, 3247 (1994).
- [10] H.C. Mastwijk, *et al.*, *Eur. Phys. J. D* **4**, 131 (1998).
- [11] N. Herschbach, *et al.*, *Phys. Rev. Lett.* **84**, 1874 (2000).
- [12] J. Léonard, *et al.*, *Phys. Rev. Lett.* **91**, 073203 (2003).
- [13] The results published in [11] by the Utrecht group have been corrected after improving the calibration of the frequency of the PA laser. The correct measurements are displayed in Table I.
- [14] J. Léonard, *et al.*, *Phys. Rev. A* **69**, 032702 (2004).
- [15] V. Venturi, *et al.*, *Phys. Rev. A* **68**, 022706 (2003).
- [16] A. J. Moerdijk, *et al.*, *Phys. Rev. Lett.* **72**, 40 (1994).
- [17] In the cases where the effective one-channel potential curves  $V_{J,\Omega_u^\pm}(r)$  don't cross each other the non-diagonal rotational couplings (between  $\Omega$  and  $\Omega \pm 1$  subspaces) can also be accounted for as a correction to these effective potentials. However, if two effective potential curves cross each other, a full multichannel calculation is needed. It turns out this situation occurs only for the effective curve  $2_u, J = 3$  which crosses  $0_u^+, J = 3$ . In this case, the non-diagonal coupling is a second order perturbation through the  $1_u$  state and we simply neglect it in our analysis, restricting ourselves to solving one-channel Schrödinger equations.
- [18] J. T. Hougen, *Nat. Bur. Stand. (U.S.), Monogr.* 115, Washington D.C., 1970.
- [19] J. Kim, *et al.*, *Eur. Phys. J. D* **32**, 227 (2004).
- [20] see *e.g.* J. Weiner, *et al.*, *Rev. Mod. Phys.* **71**, 1 (1999).
- [21] S. Seidelin, *et al.*, *Phys. Rev. Lett.* **93**, 090409 (2004).
- [22] Just before submission of this article we received a preprint of F. X. Gadéa *et al.*, in which these authors calculate the  ${}^5\Sigma_g^+$  potential and give an interpretation of the spectra reported by us earlier. The agreement with the results reported here is good.